

## Amidation and Structure Relaxation Abolish the Neurotoxicity of the Prion Peptide PrP106–126 *in Vivo* and *in Vitro*\*

Received for publication, January 6, 2005, and in revised form, April 7, 2005  
Published, JBC Papers in Press, April 11, 2005, DOI 10.1074/jbc.M500210200

Ann-Louise Bergström‡§, Henriette Cordes‡, Nicole Zsurger¶, Peter M. H. Heegaard‡, Henning Laursen||, and Joëlle Chabry¶

From the ‡Danish Institute for Food and Veterinary Research, Department of Veterinary Diagnostics and Research, Bülowsvej 27, 1790 Copenhagen V, Denmark, ¶Institute de Pharmacologie Moléculaire et Cellulaire, CNRS, Unité Mixte de Recherche 6097, 660 Route des Lucioles, Sophia Antipolis, 06560 Valbonne, France, and the ||Laboratory of Neuropathology, Rigshospitalet, 2100 Copenhagen Ø, Denmark

One of the major pathological hallmarks of transmissible spongiform encephalopathies (TSEs) is the accumulation of a pathogenic (scrapie) isoform (PrP<sup>Sc</sup>) of the cellular prion protein (PrP<sup>C</sup>) primarily in the central nervous system. The synthetic prion peptide PrP106–126 shares many characteristics with PrP<sup>Sc</sup> in that it shows PrP<sup>C</sup>-dependent neurotoxicity both *in vivo* and *in vitro*. Moreover, PrP106–126 *in vitro* neurotoxicity has been closely associated with the ability to form fibrils. Here, we studied the *in vivo* neurotoxicity of molecular variants of PrP106–126 toward retinal neurons using electroretinographic recordings in mice after intraocular injections of the peptides. We found that amidation and structure relaxation of PrP106–126 significantly reduced the neurotoxicity *in vivo*. This was also found *in vitro* in primary neuronal cultures from mouse and rat brain. Thioflavin T binding studies showed that amidation and structure relaxation significantly reduced the ability of PrP106–126 to attain fibrillar structures in physiological salt solutions. This study hence supports the assumption that the neurotoxic potential of PrP106–126 is closely related to its ability to attain secondary structure.

Prion diseases or transmissible spongiform encephalopathies (TSEs)<sup>1</sup> represent a group of fatal, neurodegenerative diseases including *e.g.* Creutzfeldt-Jakob disease in humans, scrapie in sheep and goats, chronic wasting disease in deer, and bovine spongiform encephalopathy in cattle. The etiology of the diseases can be sporadic, hereditary, or infective. According to the “protein-only” hypothesis (1), the basic infectious mechanism is thought to be a conformational change of the normal (cellular) prion protein (PrP<sup>C</sup>) into the pathogenic (scrapie) PrP<sup>Sc</sup> catalyzed by PrP<sup>Sc</sup> itself. Thus, presence of PrP<sup>C</sup> is a prerequisite for prion infection (2).

PrP<sup>C</sup> is a glycosylphosphatidylinositol-anchored glycoprotein constitutively expressed on the surface of primarily neuronal cells. It consists of two structurally different parts, namely a

C-terminal, globular part mainly  $\alpha$ -helical in nature and an unstructured, N-terminal part (3, 4). Misfolding of PrP<sup>C</sup> into PrP<sup>Sc</sup> occurs post-translationally and results in increased  $\beta$ -sheet content and a gain of protease resistance. The central region of PrP<sup>C</sup> linking the unstructured N-terminal part with the globular C-terminal domain is believed to play a pivotal role in these conformational changes (5–8).

The pathological hallmarks of the TSEs, which are mainly restricted to the central nervous system, include deposition of PrP<sup>Sc</sup>, vacuolization of gray matter, neuronal death, and neuroinflammation manifested as astrogliosis and activation of microglia cells (9, 10). Normally, PrP<sup>Sc</sup> deposition and neuropathology are spatiotemporally correlated *in vivo* (11–13); however, examples of the uncoupling of these events have been reported (14). The molecular mechanism of TSE-associated cell death is poorly understood, although it seems that apoptosis is involved (reviewed by Hetz *et al.* (15) and Liberski *et al.* (16)). Up-regulation of pro-apoptotic markers has been found in post-mortem brains from Creutzfeldt-Jakob disease patients (17) and has additionally been found to precede the accumulation of PrP<sup>Sc</sup> in scrapie-infected mice (18). The exact nature of the neurotoxic entity in the TSEs is still debated. Cytotoxicity of purified PrP<sup>Sc</sup> has been shown in PrP<sup>C</sup>-expressing neuroblastoma cells *in vitro* (15); however whether large aggregates or smaller oligomers of PrP<sup>Sc</sup> are toxic is unknown (19).

A synthetic peptide named PrP106–126 (numbering corresponding to the human prion protein sequence) resides within the central region of PrP near the N-terminal of the protease-resistant part of PrP<sup>Sc</sup>. PrP106–126 shares many properties with PrP<sup>Sc</sup>, as it readily forms amyloid fibrils with a high  $\beta$ -sheet content (20), shows partial proteinase K resistance (20, 21), and is neurotoxic both *in vivo* (22, 23) and *in vitro* (23–28). PrP106–126 contains the palindrome sequence AGAAAAGA, which makes it highly amyloidogenic. In contrast to other synthetic prion protein fragments that induce neuronal death independently of PrP<sup>C</sup> expression (23, 29), the neurotoxicity of PrP106–126 depends on the expression of endogenous PrP<sup>C</sup> (23), which makes PrP106–126 a relevant model for PrP<sup>Sc</sup> neurotoxicity. The *in vivo* neurotoxicity has been proposed to be linked to its aggregate-forming behavior and ability to form secondary structure in an aqueous environment (22). PrP106–126 causes neuronal death via induction of apoptosis (15, 22, 23), and events such as mitochondrial disruption (30), oxidative stress (31), and activation of caspases (15) have been found to be involved in this process. Also, another prion-derived peptide, PrP118–135, has been found to cause neuronal death via induction of apoptosis (23). The toxicity of PrP118–135 is, however, independent of endogenous PrP<sup>C</sup> expression. The toxicity of PrP106–126 has been found to be enhanced by activation of

\* The costs of publication of this article were defrayed in part by the payment of page charges. This article must therefore be hereby marked “advertisement” in accordance with 18 U.S.C. Section 1734 solely to indicate this fact.

§ To whom correspondence should be addressed. E-mail: alb@dfvf.dk.

<sup>1</sup> The abbreviations used are: TSE, transmissible spongiform encephalopathy; CGN, cerebellar granular neurons; DAB, 3,3'-diaminobenzidine tetrachloride; dpi, days post injection; ECN, embryonal cortical neuron; ERG, electroretinography; MTS, 3-(4,5-dimethylthiazol-2-yl)-5-(3-carboxymethoxyphenyl)-2-(4-sulfophenyl)-2H-tetrazolium; PBS, phosphate-buffered saline; PrP<sup>C</sup>, cellular prion protein; PrP<sup>Sc</sup>, scrapie prion protein; ThT, thioflavin T; TUNEL, terminal deoxynucleotidyl-transferase-mediated dUTP nick end labeling.

microglia cells (27) and astrocytes (25).

The neuroretina represents an easily accessible and fully integrated part of the central nervous system. Normally, there is a very low level of protease activity in the corpus vitreum of young, healthy animals (32), and injections of peptides can be made directly into the posterior chamber of the eye without causing damage to the eye. The neuronal cells of the retina express PrP<sup>C</sup> (33, 34) and are sensitive to PrP106–126 neurotoxicity, whereas the retinal neurons of PrP<sup>-/-</sup> mice are resistant to this effect (23). Damage to retinal cells can be quantified with electroretinographic recordings.

We recently showed that C-terminal amidation and structure relaxation of PrP106–126 significantly reduced the peptide's ability to form amyloid structure in water (35). Amidation of the C terminus has also been indicated by others to induce random coil structure in the peptide and to decrease its propensity to form amyloid fibrils (28).

Here, we found that amidation and structure relaxation of the PrP106–126 significantly reduced the peptide's *in vivo* and *in vitro* neurotoxicity and reduced its ability to form amyloid fibrils in a physiological salt solution. This finding supports the view that the fibril-forming capability of PrP106–126 is pivotal for its PrP<sup>C</sup>-dependent neurotoxicity and increases the biological relevance of this peptide as a model for PrP<sup>Sc</sup>-induced pathology.

#### MATERIALS AND METHODS

**Animals**—Adult male C57 black wild-type mice aged 9–11 weeks, were purchased from Centre d'élevage Janvier (Le Genest St Isle, France) or from Harlan Scandinavia (Allerød, Denmark). PrP<sup>-/-</sup> mice named Zurich I (36) were bred in the animal facilities at the Institute de Pharmacologie Moléculaire et Cellulaire, CNRS. Wistar Hannover Galas rat pups were purchased from Taconic M&B, Ry, Denmark.

**Peptides**—Peptides were synthesized by solid phase Fmoc (N-(9-fluorenyl)methoxycarbonyl)-based synthesis using chlorotriptyl resins for peptide acids and resins with the modified Rink linker for peptide amides (Novabiochem). After synthesis, cleavage by trifluoroacetic acid was performed, and the liberated peptides were analyzed by reverse phase (C5) high performance liquid chromatography-mass spectrometry (electrospray; Shimadzu LC20) and, if necessary, purified by preparative reverse phase chromatography on Lichrosorp C18 (Merck). The following peptides were used in this work: PrP106–126 (KT-NMKHMAGAAAAGAVVGGGLG, human PrP106–126, expected  $M_r = 1912.3$ ); PrP106–126-amide (KTNMKHMAGAAAAGAVVGGGLG-amide, expected  $M_r = 1911.3$ ); scrambled control (LVGAHAGKMGANTAKAGAMVG, expected  $M_r = 1912.3$ ); and RG2-amide (KTNMKHMA-GAAAAGAVVGGGLGRGGRGG-amide, expected  $M_r = 2722$ ).

The RG2-amide sequence was designed based on the principles of peptide structure relaxation as shown by Due Larsen and Holm (37). The peptides were dissolved in sterile PBS to a concentration of 1 mM and stored in aliquots at  $-20^\circ\text{C}$  until use. For intravitreal injections and for use in the primary mouse embryonal cortical neurons, the peptides were aged for 3 days at room temperature with slight agitation. When non-aged peptides were used for injections, they were kept on ice until use. For cellular experiments with rat cerebellar granular neurons, the peptides were aged for 2 days  $37^\circ\text{C}$  at 2 mM in PBS.

**Thioflavin T (ThT) Assay for Amyloid Fibril Formation**—A thioflavin T assay was performed as described by LeVine (38). Peptides were dissolved to 1 mM in sterile PBS and allowed to incubate at room temperature with slight agitation in the presence of  $20\ \mu\text{M}$  thioflavin T (1 mM stock solution in water; Sigma T3516), reading the fluorescence each day at 485 nm using an excitation wavelength of 440 nm (with a Spectra Flour Plus microplate fluorometer from Tecan). Readings were normalized to the same gain setting to allow comparisons from sample to sample. When comparing different plates, values were further corrected for background (fluorescence of ThT in water).

**Intravitreal Injections**—Anesthesia was performed with intraperitoneal injections of pentobarbital (50 mg/kg). Topical application of a local anesthetic (Novesine®) was performed in both eyes. Injections of a  $1\text{-}\mu\text{l}$  solution were done unilaterally (in the left eye) with a 30-gauge needle introduced into the posterior chamber on the upper pole of the eye directed toward the center of the vitreous body. The injections were performed slowly (over at least 60 s) to allow diffusion of the peptide and to avoid any ocular hypertension and backflow. For electroretinography (ERG) experiments 5–10 animals were used for each treatment

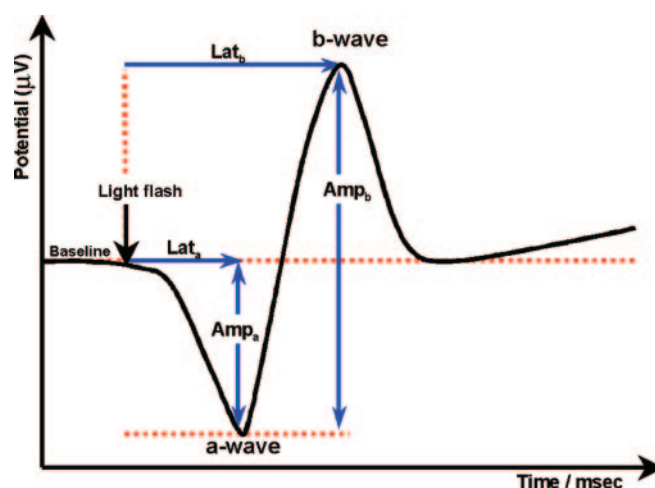


FIG. 1. **The electroretinogram.** A typical light-induced electroretinogram from a dark-adapted mouse is shown. The amplitude of the a-wave ( $Amp_a$ ) is measured from the baseline to the bottom of the a-wave, whereas the amplitude of the b-wave ( $Amp_b$ ) is measured from the bottom of the a-wave to the peak of the b-wave. The latencies of the a- and b-waves are measured as the time lag from the light flash until the bottom/peak of the waves.

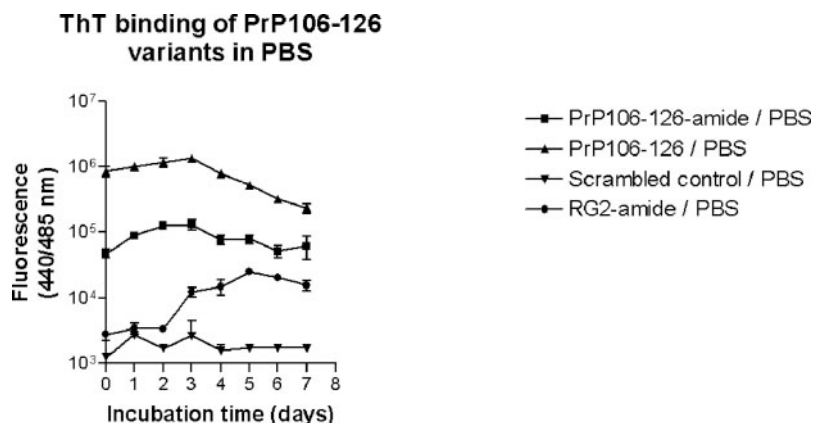
group, and for histological analyses 3–5 animals per group were used. For histological analysis of eyes at 15 days post injection (dpi), 3 mice with representative ERG values (close to the group mean) from each treatment group were selected. For histological analyses of retinas at 4 dpi, the mice were not subjected to ERG before they were killed.

**ERG Measurements and Statistical Evaluation of Effect**—Full field electroretinograms were prepared under dim red light on overnight dark-adapted animals. Anesthesia was performed with a mixture of 2% isoflurane (Forene®, Abbott Laboratories) and oxygen. The pupils of anesthetized animals were dilated with Mydraticum®. The animals were kept on a heating mat during anesthesia. A ring-shaped recording electrode was placed on the cornea of each eye, and a reference electrode was placed behind each ear. Zero electrodes were placed on the hind legs. Light stimulus (8 ms) was provided by a single flash (10 candelas/ $\text{s}^2$ ) in front of the animal. The ERGs were recorded using Win7000b (Metrovision, Pénchies, France). The amplitude of the a-wave was measured from the baseline to the bottom of the a-wave; the b-wave amplitude was measured from the bottom of the a-wave to the peak of the b-wave (Fig. 1). The averaged responses represent the mean of two white flashes (8-ms duration) delivered 2 min apart. ERGs were recorded before and then 4, 7, and 14 days after intravitreal injections. Only animals with approximately similar pre-injection values for the left and right eye were selected for injections. To quantify the effect of the injections, the non-injected eye was used as an internal control, and the absolute values for the ERG a- and b-waves of the injected eye were normalized to the non-injected control eye for each animal. Relative/normalized values for the different peptide groups were compared with the relative/normalized values for the group injected with the scrambled control peptide by using an unpaired *t* test.

**Tissue Preparation**—Mice used for ERG recordings were killed on day 15 after injection, and other groups were killed on day 4 after injection. All mice were killed by cervical dislocation. The eyes were enucleated and fixed in ice-cold 4% paraformaldehyde for a minimum of 24 h and then cryoprotected overnight in PBS containing 20% sucrose. The eyes were then embedded in TissueTek (Sakura) and frozen at  $-80^\circ\text{C}$ . Cryosections ( $10\ \mu\text{m}$ ) throughout the whole eye were cut on a cryostat. The sections were then dried for 1–2 h at  $55^\circ\text{C}$  before they were stored at  $-80^\circ\text{C}$  until further use.

**TUNEL Test on Cryosections**—A TUNEL test (Roche Applied Science *in situ* cell death detection kit, POD) was performed on frozen sections from animals 4 or 15 dpi according to the manufacturer's instructions with slight modifications. The sections were defrosted for 30 min at room temperature and then washed  $2 \times 5$  min in PBS. Blocking was performed in methanol with 3%  $\text{H}_2\text{O}_2$  for 30 min, after which the slides were washed  $2 \times 5$  min in PBS. Permeabilization was performed in  $4^\circ\text{C}$  double distilled water with 0.5% sodium citrate and 0.5% Triton X-100 followed by a short wash in PBS. A positive control was digested with DNase for 20 min at  $37^\circ\text{C}$ . A TUNEL mixture was then added to all slides (except a negative control, which received only the label solution from the TUNEL kit). Incubation with the TUNEL mixture was per-

**Fig. 2. Thioflavin T binding of peptide variants.** Thioflavin T binding of the peptides dissolved in PBS (1 mM) was analyzed by fluorescence measurements daily for 7 days. Each data point represents the mean of duplicate or quadruplicate determinations.



formed in a humid atmosphere for 3 h at 37 °C. Washing was performed 3 × 5 min in PBS at 37 °C, and a converter solution from the TUNEL kit was added to all slides. Incubation was performed for 30 min, and the slides were then washed 3 × 5 min in PBS. DAB solution (one thawed DAB tablet, Sigma catalog number D5905, dissolved in 15 ml of PBS; 12 μl of 30% H<sub>2</sub>O<sub>2</sub> was added immediately before use) was added, and development was performed for 6 min. The reaction was stopped in distilled water. The slides were dehydrated through a graded series of ethanol and mounted in xylol (Pertex). The slides were analyzed in a light microscope and photographed with a Leica DC300 digital camera.

**Primary Mouse Embryonal Cortical Neurons (ECNs) and Toxicity Assay**—Primary cortical neuronal cultures were prepared from wild type C57 black embryos. Briefly, the embryos were dissected at embryonal day 13 or 14, and the brains were extracted and rinsed from meninges in 37 °C warm Dulbecco's PBS with 1% glucose. The PBS solution was replaced by Neurobasal medium (Invitrogen) with the addition of L-glutamine, 10% inactivated fetal calf serum, B27 supplement, and penicillin/streptomycin. Gentle homogenization was performed with a Pasteur pipette, after which the cells were washed once. The cell concentration was adjusted to the appropriate concentration, and plating of 5 × 10<sup>4</sup> cells/well was performed on Nunc 96-well plates precoated overnight with poly-D-lysine. Incubation was performed at 37 °C with 5% CO<sub>2</sub> in a humidified incubator. After 30 min of incubation, the medium was changed. After 24 h of incubation, the medium was replaced by serum-free Neurobasal medium with a B27 supplement, L-glutamine, and penicillin/streptomycin. Peptides were added after 3–5 days of maturation and incubated for 12, 24, and 48 h. Viability was measured with an MTS assay (CellTiter96, Aqueous One solution cell proliferation assay; Promega). A<sub>492 nm</sub> was measured on a spectrophotometer.

**Primary Rat Cerebellar Granular Neurons (CGNs) and Toxicity Assay**—CGNs were isolated from 7–8 day-old Wistar Hannover Galas rat pups (Taconic M&B) as described by Patel & Kingsbury (39) with some modifications. Briefly, cerebellar granules were isolated from pups after decapitation. The tissue was suspended in Krebs buffer and digested with trypsin before single cell suspensions were made in Neurobasal A medium supplemented with 10% fetal calf serum, 35 mM KCl, GlutaMAX-I supplement, penicillin/streptomycin, and 1 mM sodium pyruvate (Invitrogen). The cell concentration was adjusted to the appropriate concentration, and plating of 8 × 10<sup>4</sup> cells/well was performed on 96-well plates precoated with poly-D-lysine (BD Biosciences) and incubated for 2 h at 37 °C and 5% CO<sub>2</sub> in a humidified incubator. The medium was changed to serum-free Neurobasal A with B27 (without antioxidants) and the same supplements as above. On day 6 the medium was replaced by fresh Neurobasal A (without phenol red) with the addition of B27 (without antioxidants), the same supplements as above, and peptides to a final concentration of 100 μM. Viability was measured day 15 using the WST-1 assay as described in the manufacturer's manual (cell proliferation reagent WST-1; Roche Applied Science). The cells were analyzed in light microscope and photographed with a Leica DC300 digital camera after 9 days of treatment.

**Caspase Induction**—CGNs were isolated as described above and incubated for 6 days before peptides were added in serum-free Neurobasal A medium (without antioxidants, supplemented with 15 mM KCl and B27) in 96-well black microtiter plates (Optilux, BD Biosciences) precoated with poly-D-lysine. After incubation for 3 days, the induction of caspases was measured in a cell lysate described in the manufacturer's manual (homogenous caspases assay, Roche Applied Science). This assay measures mainly caspase-2, -3, and -7.

**Immunocytochemistry on CGN**—CGN cultures were grown at 37 °C with 5% CO<sub>2</sub> on eight-chamber Lab-Tek Permanox chamber slides (Nalge Nunc) precoated with poly-D-lysine. The cells were fixed in 4% paraformaldehyde in PBS, pH 7.4 (freshly prepared overnight with stirring), for 1 h at room temperature and washed with washing buffer (1% Triton X-100 in PBS, pH 7.4) 3 × 5 min with gentle agitation before incubating overnight at 4 °C with 1 μg/ml of the mouse monoclonal anti-PrP antibody SAF32 (Spi-Bio, Montigny le Bretonneaux, France) or mouse IgG2b (catalog number X0944, DAKO) diluted in PBS, pH 7.4, with 1.5% horse serum. After rinsing, the slides were incubated with biotinylated anti-mouse immunoglobulin antibody diluted 1:200 in PBS, pH 7.4, with 1.5% horse serum for 1 h at room temperature, rinsed, and incubated with ABC reagent for 30 min (antibodies and ABC-reagent Vectastain ABC kit from Vector Laboratories). After rinsing, slides were developed with a DAB solution (one thawed DAB tablet from Sigma was diluted in 15 ml PBS; 12 μl of H<sub>2</sub>O<sub>2</sub> was added immediately before use) before rinsing in distilled water. Slides were mounted with Aquamount mounting media (BDH Laboratories, Poole, UK) under glass coverslips.

## RESULTS

**Amidation and Structure Relaxation of PrP106–126 Reduce Its Tendency to Form Amyloid Fibrils in PBS**—We analyzed the fibrillation tendency (amyloidogenicity) of the peptides at 1 mM in PBS with the ThT assay where fluorescence was followed for 7 days (Fig. 2). Fibrillation of PrP106–126 in PBS peaked after 3 days of incubation, after which it started to decline. The PrP106–126-amide and the RG2-amide showed much lower fibrillation tendency compared with PrP106–126, although they both rose to levels significantly higher than the scrambled control peptide. The fibrillation of the RG2-amide proceeded slower than that of both PrP106–126 and PrP106–126-amide, peaking after 5 days of incubation as opposed to 3 days of incubation.

**Fibrillar PrP106–126 Induces Long Term Changes in the Retina**—To test the peptide variants for their *in vivo* neurotoxicity, we performed intravitreal injections of the 3-day-aged peptides and performed ERG recordings at 4, 7, and 14 dpi. All animals were injected in their left eye only (the right was left as non-injected or PBS-injected controls). No difference was observed between non-injected and PBS-injected eyes (data not shown). Both eyes were measured by ERG, and for each animal the absolute values of the ERG a- and b-waves, respectively, for the injected eye were normalized to the control eye values (the a-wave and b-wave amplitude values from the control eye was set to 100%). This was done to avoid time-to-time variation in the ERG due to its sensitivity to variable factors like anesthesia, room temperature, circadian time, electrical noise, etc. All ERG-wave values are therefore represented as a percentage of control values. Because none of the tested peptides induced significant changes in the latency of either the a-wave nor the b-wave at any time point, this study focuses on the amplitude of these waves only. All of the ERG results are represented in Table I.

TABLE I  
ERG responses after intraocular injections of peptides

Electroretinograms were recorded on overnight dark-adapted animals before (not shown) and then 4, 7, and 14 days after intraocular injections of the peptide variants (aged for 3 days at room temperature). The a-wave and b-wave values are normalized to uninjected control eye values and shown as mean percentage  $\pm$  S.E. of the respective groups ( $n = 5$ –10).

Peptide	4 dpi		7 dpi		14 dpi	
	a-wave	b-wave	a-wave	b-wave	a-wave	b-wave
PrP106–126 (aged)	86.10 $\pm$ 7.19	81.03 $\pm$ 4.86	85.3 $\pm$ 6.5	86.54 $\pm$ 4.32	82.36 $\pm$ 8.45	82.21 $\pm$ 4.34
PrP106–126-amide (aged)	107.9 $\pm$ 7.09	95.10 $\pm$ 4.20	94.36 $\pm$ 4.07	90.92 $\pm$ 3.06	95.4 $\pm$ 7.07	94.55 $\pm$ 4.69
RG2-amide (aged)	100.8 $\pm$ 1.85	92.18 $\pm$ 5.76	96.11 $\pm$ 5.12	98.51 $\pm$ 8.62	89.28 $\pm$ 5.82	87.19 $\pm$ 5.72
Scrambled control (aged)	97.87 $\pm$ 3.43	98.98 $\pm$ 3.52	103.2 $\pm$ 4.25	99.14 $\pm$ 2.93	95.47 $\pm$ 2.79	102.4 $\pm$ 2.24

Injection of a 3-day-aged solution (1 mM) of the scrambled control peptide did not induce a-wave or b-wave amplitude values significantly different from those of the non-injected control eyes at any of the time points tested. The ERG values obtained with the other peptides were therefore tested statistically against the values obtained with the scrambled control peptide.

Injection of a 3-day-aged solution of the PrP106–126 peptide resulted in relative b-wave values that were significantly reduced compared with the corresponding values from the scrambled control group at 4 dpi (17.96%,  $p = 0.006$ ), 7 dpi (12.6%,  $p = 0.02$ ), and 14 dpi (20.22%,  $p = 0.0007$ ). For the a-wave, the values for the PrP106–126 (aged) group were significantly lower than the scrambled control group only at 7 dpi (17.88%,  $p = 0.027$ ), although there was a tendency for the a-wave to be reduced at 4 dpi (11.77%,  $p = 0.14$ ) and 14 dpi (13.11%,  $p = 0.16$ ). Injection of a fresh solution of PrP106–126 yielded a significant reduction of the b-wave (15.87%,  $p = 0.046$ ) and a non-significant tendency of the a-wave to be reduced (15.79%,  $p = 0.072$ ) at 4 dpi, only. At 7 dpi there was no reduction of either the a-wave or the b-wave with the freshly dissolved peptide (data not shown). Injection of the aged PrP106–126 had no significant effect on ERG in PrP<sup>0/0</sup> mice (data not shown).

**Amidation Diminishes the *in Vivo* Neurotoxicity of PrP106–126**—To correlate fibrillation propensity with *in vivo* neurotoxicity, we injected an amidated variant of the PrP106–126 (PrP106–126-amide). Injection of a 3-day-aged solution of this peptide had no significant effect on either the b-wave or the a-wave at any time point (Table I). A fresh solution of the PrP106–126-amide had no significant effect on either the a-wave or the b-wave at any time point (data not shown).

**Structure Relaxation and Amidation Reduces the *in Vivo* Neurotoxicity of PrP106–126**—Injection of a 3-day-aged solution of the structure-relaxed and amidated variant of PrP106–126 (RG2-amide) resulted in no significant reduction of the b-wave at 4 or 7 dpi, but at 14 dpi there was a significant reduction compared with the scrambled group (15.23%,  $p = 0.012$ ), as shown in Table I. There was no significant reduction of the a-wave at any time point with this peptide. A fresh solution of the RG2-amide had no significant effect on either the a-wave or the b-wave at any time point (data not shown).

**Spatiotemporal Correlation of Apoptotic Cell Death and ERG Effect**—To correlate the effect observed on the electroretinograms to apoptotic cell death, we performed histological analyses on retinal sections from injected eyes at 4 and 15 dpi. Four days after injection of the aged PrP106–126, TUNEL-positive nuclei were detected primarily in the retinal ganglion cell layer (Fig. 3B). In the mice injected with the scrambled peptide, only very sparsely distributed TUNEL-positive cells were detected in the outer nuclear layer at 4 dpi (Fig. 3A). At day 15 after injection with the aged PrP106–126, TUNEL-positive nuclei were detected in all nuclear layers of the retina (Fig. 3F), and a disruption of the ganglion cell layer could be identified (Fig. 3F). Injection of the scrambled control peptide yielded no de-

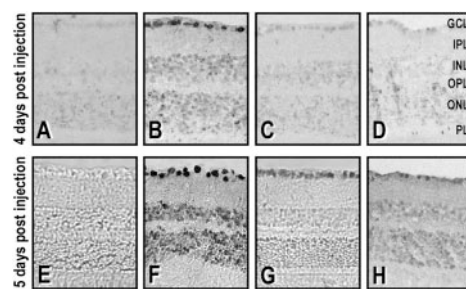


FIG. 3. TUNEL test on retinal sections after intraocular injections of aged peptide solutions. Dark nuclei represent cells with detectable DNA fragmentation. A, scrambled control peptide, 4 dpi. B, PrP106–126, 4 dpi. C, PrP106–126-amide, 4 dpi. D, RG2-amide, 4 dpi. E, scrambled control peptide, 15 dpi, shown with phase contrast. F, PrP106–126, 15 dpi. G, PrP106–126-amide, 15 dpi. H, RG2-amide, 15 dpi. All photomicrographs are shown at 400 $\times$  magnification. GCL, ganglion cell layer; INL, inner nuclear layer; IPL, inner plexiform layer; ONL, outer nuclear layer; OPL, outer plexiform layer; PL, photoreceptor layer.

tectable TUNEL-positive nuclei at 15 dpi (Fig. 3E). Interestingly, in mice injected with fresh solutions of the PrP106–126, no TUNEL-positive nuclei were detected in the ganglion cell layer at either 1 or 4 dpi, whereas a significant amount was detected in the outer nuclear layer at both of these time points (Fig. 4, E and F). The same pattern was observed at 1 dpi with the aged PrP106–126 (Fig. 4G).

The PrP106–126-amide did not induce TUNEL-positive nuclei at 4 dpi (Fig. 3C), whereas at 15 dpi some weakly TUNEL-positive nuclei could be detected in the ganglion cell layer (Fig. 3G). Injection of the RG2-amide resulted in some weakly TUNEL-positive cells in the ganglion cell layer and the inner nuclear layer at 4 dpi (Fig. 3D). This effect was even more pronounced at 15 dpi (Fig. 3H).

**Cytotoxicity in Primary Neurons Supports *in Vivo* Results**—The short term neurotoxicity of the PrP106–126 variants was tested in primary murine ECNs. For this test the peptides were aged under the same conditions as those used for intravitreal injections (3 days at room temperature). The cells were incubated with the different peptides at the concentrations 40, 80, and 160  $\mu$ M for 24 and 48 h. PrP106–126 had a time- and concentration-dependent effect on cell viability (Fig. 5A), whereas the PrP106–126-amide showed only a weak tendency to be toxic after 48 h of treatment with 160  $\mu$ M (Fig. 5B). The RG2-amide and the scrambled control peptide showed no significant toxicity in this system (Fig. 5, C and D, respectively).

The long term neurotoxic effect *in vitro* was tested in another cellular system (rat CGNs). Immunocytochemistry on these cells revealed that PrP<sup>C</sup> was expressed on both the soma and the axons of the cells (Fig. 6E). In this setup, peptides were added to the cells 6 days after plating and left to incubate for 9 days. Initial experiments showed that pre-aging the peptides for 2 days in PBS actually reduced their toxicity in this system compared with addition of freshly dissolved peptides (Table II).

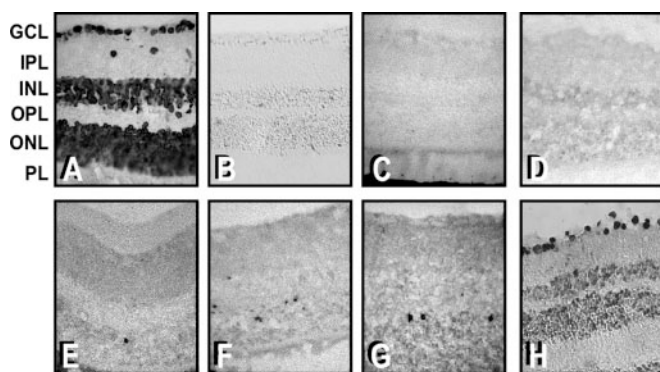


FIG. 4. TUNEL test on retinal sections. A, positive control (DNase-treated). B, negative control (no enzyme added to the TUNEL reaction) shown with phase contrast. C, 1 dpi after intraocular injection of isotonic saline. D, 4 dpi after injection of isotonic saline. E, 1 dpi after injection of freshly dissolved PrP106–126. F, 4 dpi after intraocular injection of freshly dissolved PrP106–126. G, 1 dpi after injection of aged PrP106–126. H, 4 dpi after injection of aged PrP106–126. All photomicrographs are shown at 400 $\times$  magnification. GCL, ganglion cell layer; INL, inner nuclear layer; IPL, inner plexiform layer; ONL, outer nuclear layer; OPL, outer plexiform layer; PL, photoreceptor layer.

Therefore, we decided to use freshly dissolved peptides, expecting that the peptides would aggregate during the 9 days of incubation with the cells. Incubation with 100  $\mu$ M PrP106–126 resulted in a significant reduction in viability compared with controls (56%). Cells treated with 100  $\mu$ M PrP106–126-amide form or the scrambled control peptide showed no significant reduction in viability after 9 days of treatment (Table II).

**Morphological Changes in CGNs Treated with PrP106–126**—Nine days of treatment with the PrP106–126 peptide induced clear morphological changes in the CGNs (several shrunken cells, Fig. 6A). Slight morphological changes could be seen after 9 days of incubation with either the PrP106–126-amide or the RG2-amide, as some sparsely distributed shrunken cells could be observed (Fig. 6, B and C), although neither of these peptides resulted in measurable reductions in viability. No morphological changes could be observed in the cells treated with the scrambled control peptide (Fig. 6D).

**Caspase Induction in CGN**—The ability of the peptides to induce general caspase activity was tested in the CGN cultures. Three days of incubation with PrP106–126 (100  $\mu$ M) resulted in an increased level of general caspase activity ( $\approx$ 35%) compared with control media levels (Fig. 7). The toxin camptothecin (a DNA topoisomerase I inhibitor) induced a caspase activity level that was  $\approx$ 50% above that of the media control. Incubation with the RG2-amide resulted in a  $\approx$ 30% increase, whereas both the PrP106–126-amide and the scrambled control peptide resulted in levels of caspase activity close to the media control levels. Only the PrP106–126 and the camptothecin-induced caspase levels that were significantly increased compared with that of the scrambled control peptide (unpaired *t* test).

#### DISCUSSION

Most of previous work with PrP106–126 utilized the unmodified acid form of the peptide, *i.e.* the peptide with a free C-terminal carboxylate group, although this is rarely indicated precisely. As shown here and previously (28, 35), the amyloidogenicity of the free PrP106–126 peptide differs greatly from that of the PrP106–126-amide, and, as a whole, the amyloidogenicity of PrP106–126 is very sensitive to minor molecular modifications including oxidation, structure relaxation, and stabilization (35). The delicate nature of PrP106–126 could explain some of the contradictory findings reported on the neurotoxicity of this peptide (40–42). We therefore wanted to study the possible effects of a minor modification (C-terminal

amidation) on the toxicity of the PrP106–126 peptide. Amidation is clearly biologically relevant considering the location of PrP106–126 internally in the PrP polypeptide.

We found that the ability to form amyloid fibrils was closely correlated with the neurotoxicity of PrP106–126, as amidation reduced both the amyloidogenicity and neurotoxicity of the peptide. Many other synthetic peptides similarly show fibrillogenic and neurotoxic properties, but PrP106–126 is unique in that it requires the expression of endogenous PrP<sup>C</sup> to exert its toxicity. This parallels the action of PrP<sup>Sc</sup> (15, 43) and makes PrP106–126 an excellent model for TSE pathogenesis. There are several advantages of using PrP106–126 instead of PrP<sup>Sc</sup> itself. First, the biological effects of molecular modifications can easily be studied, and, second, the PrP<sup>Sc</sup> preparations are never completely pure and contain other proteins, lipids, carbohydrates, nucleic acids, and traces of metals and detergents that could interfere with the measurements (44).

Other PrP-derived peptides seem to exert their toxicity through general cytotoxic mechanisms shared with other, non-PrP-derived peptides such as A $\beta$ 1–42,  $\alpha$ -synuclein, and the islet amyloid polypeptide. Much evidence indicates that these mechanisms involve perturbation of membrane integrity and oxidative stress that do not rely on the presence of mature fibrils but rather on the formation of soluble oligomers with fusogenic properties (45). For instance, the PrP-derived peptides PrP105–132 and PrP118–135 are able to insert into and perturb the integrity of the cell membrane of both PrP-expressing and PrP<sup>-/-</sup> cells (23, 29). The toxicity of PrP105–132 and PrP118–135 is thus independent of PrP<sup>C</sup>-expression and amyloid fibril formation. This may be relevant to the *in vivo* neuropathogenic process involved in rare cases of TSEs such as Gerstmann-Sträussler-Scheinker disease, but it cannot be taken as a general mechanism.

The correlation between secondary structure and PrP<sup>C</sup>-dependent toxicity of PrP106–126 indicates that a well defined conformation of the peptide is a prerequisite for the interaction with a specific cell component leading to toxicity. A probable scenario is that this conformation is necessary for the peptide to be able to form fibrils and that these fibrils or their precursors are responsible for the neurotoxic binding to a specific cellular receptor. Several other PrP-derived peptides are able to form fibrils showing PrP<sup>C</sup> independent neurotoxicity (23, 29, 56), indicating that PrP<sup>C</sup> has no indispensable role in neurotoxicity caused by peptide fibrillation. It is therefore probable that the specific PrP<sup>C</sup>-dependent neurotoxic effect of PrP106–126 simply implicates PrP<sup>C</sup> itself as the cellular receptor and relies on a complex being formed between adequately aggregated PrP106–126 and PrP<sup>C</sup>. This would, in turn, depend on a precisely defined conformation of PrP106–126.

The ThT binding studies discussed here showed that PrP106–126 easily formed amyloid fibrils in PBS, peaking after only a few days of aging. It is interesting that the fibrillation process proceeded much faster and reached much higher levels in PBS than those found previously in pure water (35). As expected, both the amidated and the RG2-amide variant of PrP106–126 showed much less ability to form amyloid fibrils than the acid variant; however, they both reached ThT binding levels well above those of the scrambled control peptide. This was not discernible in water, where both the PrP106–126-amide and RG2-amide showed ThT fluorescence at the level of the scrambled control peptide (35).

In accordance with previously reported findings (22, 23), we found that the acid form of PrP106–126 was neurotoxic both *in vivo* and *in vitro*. The magnitude of the reduction of the ERG wave amplitudes we report here are smaller than those reported previously. This could be explained by the differences in

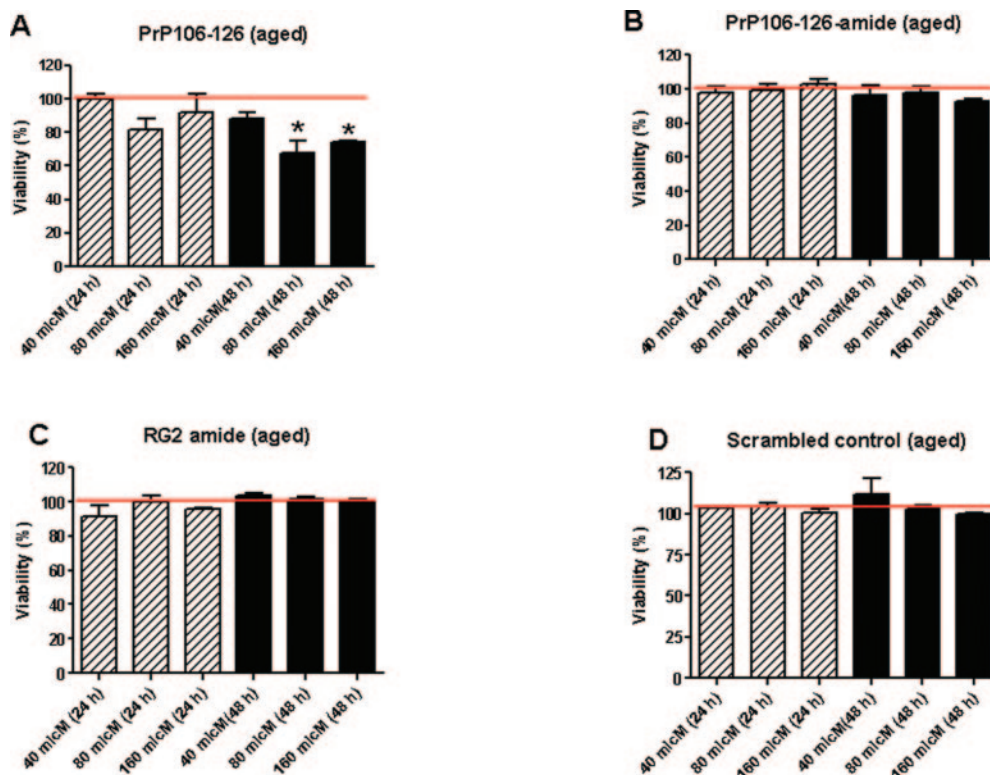


FIG. 5. Viability of mouse embryonal cortical neurons after incubation with aged peptide solutions (absorbance at 492 nm after 2–4 h of incubation with MTS). The values are shown as the percentage of media control (mean  $\pm$  S.E.). The peptides were tested in three different concentrations, 40, 80, and 160  $\mu$ M and incubated for either 24 or 48 h. The values are obtained by three independent experiments. Asterisks indicate values that are significantly different from those of the media control.

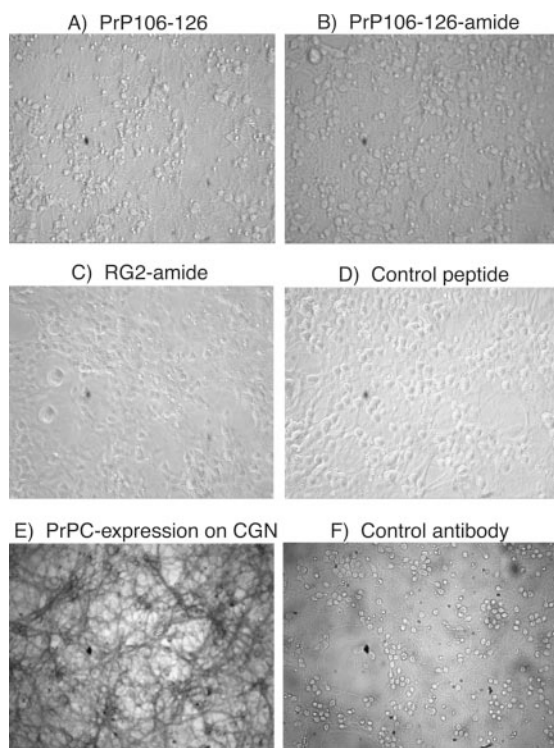


FIG. 6. Morphological changes in cerebellar granular cells after treatment with PrP106–126-acid peptides, and the expression of PrP<sup>C</sup> on CGN cultures. A–D, CGNs were incubated for 9 days (from day 6 to day 15) with 100  $\mu$ M of PrP106–126 (A), PrP106–126-amide (B), PrP106–126-RG2-amide (C), or scrambled control peptide (D). E and F, expression of PrP<sup>C</sup> on the CGN cultures. The CGN cultures were immunostained with anti-PrP mAb SAF32 (E) or mouse IgG2b control antibody (F). All photomicrographs are shown at 400 $\times$  magnification.

TABLE II  
Effect of PrP peptides on CGN viability

CGNs were isolated from rat cerebellar granules and left to differentiate for 6 days before the addition of PrP peptides (100  $\mu$ M) or the control compound camptothecin (20  $\mu$ M). After long-term incubation (9 days), cell viability was measured using a WST-1 assay. Results are given as the percentage of viability of media controls.

Compound	Viability
	%
Camptothecin	30 $\pm$ 9
PrP106–126-acid	56 $\pm$ 11
PrP106–126-acid (aged)	85 $\pm$ 10
PrP106–126-amide	$\sim$ 100 $\pm$ 29
PrP106–126 RG2-amide	$\sim$ 100 $\pm$ 22
Scrambled peptide	$\sim$ 100 $\pm$ 13

experimental and statistical methods. Previously, the effect of the peptides was calculated by comparing the absolute ERG values before and after injection in the same eye (22, 23). We found that the response of the normal ERG tended to be suppressed by repeated inductions of anesthesia, which could potentially increase the observed effect. Furthermore, the ERG was very sensitive to factors like circadian time, room temperature, and electrical noise. To correct for such variations in the absolute values of the ERG, we normalized the absolute values of the injected eyes to the control eyes. As we found that injections of isotonic saline, PBS, or the scrambled control peptide had no effect on the ERG, we do not expect this to add any bias to the experimental design.

The results in both cellular systems (CGNs and ECNs) support the *in vivo* results, as the unmodified, acid form of PrP106–126 was found to show a time- and concentration-dependent toxicity. We found the toxic effect to be significant and reproducible in both a short term setup (24 and 48 h of treatment in the ECNs) and a long term setup (9 days of treatment in the CGNs).

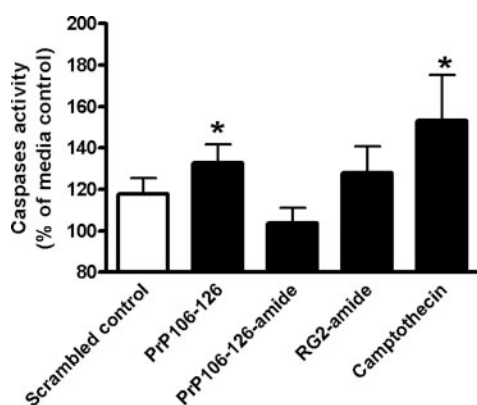


FIG. 7. **Induction of caspase activity in CGN.** The CGN cultures were incubated for 3 days with of peptides (100  $\mu\text{M}$ ) or camptothecin (20  $\mu\text{M}$ ). The general caspase activity is given as a percentage of media control (mean  $\pm$  S.E.). Asterisks indicate values that are significantly different from those of the scrambled control peptide.

Amidation of PrP106–126 diminished the neurotoxic effect both *in vivo* and *in vitro* significantly. The PrP106–126-amide did not induce significant ERG changes or apoptotic cell death in the retina after intraocular injections. Likewise, there was no effect on viability or apoptosis induction in neuronal cell cultures. In contrast, Salmona *et al.* (28) showed that although C-terminal amidation of PrP106–126 increases the random coil structure and reduces its ability to induce astroglia proliferation, it did not interfere with the peptide's neurotoxic potential toward rat cortical neurons. This discrepancy could be explained by the fact that Salmona *et al.* added the peptides to the embryonal rat cortical neurons 1 day after plating and then treated the neurons for 7 days. We added the peptides several days after plating in both cellular systems (3–4 days for the ECN and 6 days for the CGN), and it is thus possible that the less matured neuronal cultures in the experiments of Salmona *et al.* were more sensitive to peptide toxicity and hence showed increased susceptibility to the amidated PrP106–126 than our cultures. This view is furthermore supported by the fact that Salmona *et al.* reported larger effects on viability with the PrP106–126 (acid variant) peptide than we did.

With regard to the structure-relaxed and amidated RG2-peptide (with the addition of large basic groups C-terminally), it showed a level of toxicity more or less on the same level as that of the PrP106–126-amide. However, there was a slight reduction of the ERG b-wave at 14 dpi *in vivo* (and some TUNEL-positive cells in the retina at 15 dpi). In the ECN cultures we could not detect significant cell death after 24 or 48 h of treatment with the RG2-amide peptide. In the CGN cultures, however, although we did not detect significant cell death after 9 days of treatment with the RG2-amide, we did see slight morphological changes that could not be seen with either the PrP106–126-amide or the scrambled control peptide. We observed a moderate increase in the general caspase activity in the CGN cultures 3 days after the addition of the RG2-amide, but this was also observed with the scrambled control peptide. Caspase activation may, however, not always indicate cell death, as there are several examples of uncoupling, especially of caspase-3 activity and apoptotic cell death (46, 47).

The effect of the structure relaxation due to the addition of the RG2 group could not be fully evaluated, as the amidated variant of the RG2-peptide was used here. To investigate this effect, the acid variant of the RG2 peptide should be used. We recently published a report demonstrating that the RG2 acid variant shows significantly reduced ability to form amyloid fibrils in water as assayed by ThT binding (35). We are cur-

rently performing toxicity experiments with the RG2 acid variant to clarify if this reduced tendency to form amyloid fibrils correlates with reduced neurotoxicity.

The effect of the aged PrP106–126 variant on the ERG was found to last for at least 14 days, suggesting that the observed neuronal death is not reversible. A TUNEL test performed on eyes at 15 dpi showed apoptotic nuclei in all cell layers of the retina, whereas at 4 dpi TUNEL-positive cells were mostly restricted to the ganglion cell layer (Fig. 4, B and F). Interestingly, we observed that TUNEL-positive nuclei were restricted to the outer nuclear layer in mice killed at 1 dpi or 4 dpi after injection of a fresh solution of PrP106–126 (Fig. 4, C and D). The same was observed 1 dpi after injection of the aged PrP106–126 (Fig. 4G). As the outer nuclear layer mostly consists of photoreceptors, this finding could indicate that photoreceptors are more susceptible to prion peptide toxicity than the other cell types of the retina (*e.g.* bipolar and ganglion cells). In hamsters infected with experimental scrapie, photoreceptor degeneration is the earliest and most profound retinopathological finding (48–50). Similarly, in mice infected with the 79A strain of scrapie, apoptosis and degeneration of the outer nuclear layer were observed at the onset of clinical disease (33). Other strains of scrapie in mice likewise induce retinopathy, with the most prominent pathological changes localized to the photoreceptors (51, 52).

Labeling of PrP mRNA in C57/BL6-mice was found in all cell types of the retina, although most intensively in the photoreceptor layer (33). In concordance with this finding, Chishti *et al.* (34) found that expression of hamster PrP<sup>C</sup> in the retina of hamster and transgenic mice was most pronounced in the photoreceptor layer. It is possible that the high expression of PrP<sup>C</sup> on the photoreceptor cells renders them more vulnerable to prion peptide and PrP<sup>Sc</sup> toxicity. Accumulation of PrP<sup>Sc</sup> in the retina seems mainly to be located in the plexiform layers (in humans with Creutzfeldt-Jakob disease (53) and scrapie-infected hamsters (54)), reflecting a synaptic accumulation. We similarly performed immunohistochemistry and a paraffin-embedded tissue blot on retinas from 263K-infected hamsters and found the accumulation to be particularly prominent in the plexiform layers.<sup>2</sup>

ThT binding indicates formation of amyloid fibrils (38), representing the end point of a multistep fibril formation pathway. Here, we found a correlation between ThT binding and toxicity, but this does not preclude the possibility that toxicity derives from peptide-aggregate intermediates formed on the pathway to ThT binding fibrils, *e.g.* protofibrils, as suggested by several other studies (55). It is conceivable that the molecular variants with reduced ThT binding studied here will also have a reduced ability to form protofibrils equivalent to the reduction in fibril formation. There is, however, some controversy regarding whether PrP106–126 binds directly to PrP<sup>C</sup> or not; Gu *et al.* (57) reported a direct interaction, whereas Fioriti *et al.* (58) found that PrP106–126 exerted its effect without interacting directly with PrP<sup>C</sup>. A precisely defined conformation and a direct interaction with PrP<sup>C</sup> are both hallmarks of PrP<sup>Sc</sup> neurotoxicity (15, 43).

In conclusion, we found that the PrP<sup>C</sup>-dependent neurotoxicity of the PrP106–126 peptide was closely related to its ability to form fibrillar structures in aqueous solution, as structural changes interfering with this ability abolished the neurotoxicity of the peptide. This was found to be significant both *in vivo* and in two different primary neuronal systems. We are currently investigating how other small molecular changes, similarly shown to interfere with the fibrillation process (*e.g.* oxi-

<sup>2</sup> A.-L. Bergström, H. Laursen, and P. Lind, unpublished results.

ation), will affect the PrP<sup>C</sup>-dependent neurotoxicity of the PrP106–126 peptide.

**Acknowledgments**—The skillful technical assistance of Heidi Gertz Pedersen, Pia Vest, and Jean-Daniel Barde is gratefully acknowledged. Peter Lind, Vivi Bille-Hansen, and Yang Sun Bøg are acknowledged for critical reviews of the manuscript. Jakob Ohm is thanked for general help with technical problems.

## REFERENCES

- Prusiner, S. B., Scott, M. R., DeArmond, S. J., and Cohen, F. E. (1998) *Cell* **93**, 337–348
- Brandner, S., Raeber, A., Sailer, A., Blattler, T., Fischer, M., Weissmann, C., and Aguzzi, A. (1996) *Proc. Natl. Acad. Sci. U. S. A.* **93**, 13148–13151
- Zahn, R., Liu, A., Luhrs, T., Riek, R., von Schroetter, C., Lopez, G. F., Billeter, M., Calzolari, L., Wider, G., and Wuthrich, K. (2000) *Proc. Natl. Acad. Sci. U. S. A.* **97**, 145–150
- Lopez, G. F., Zahn, R., Riek, R., and Wuthrich, K. (2000) *Proc. Natl. Acad. Sci. U. S. A.* **97**, 8334–8339
- Muramoto, T., Scott, M., Cohen, F. E., and Prusiner, S. B. (1996) *Proc. Natl. Acad. Sci. U. S. A.* **93**, 15457–15462
- Rogers, M., Yehiely, F., Scott, M., and Prusiner, S. B. (1993) *Proc. Natl. Acad. Sci. U. S. A.* **90**, 3182–3186
- Chabry, J., Caughey, B., and Chesebro, B. (1998) *J. Biol. Chem.* **273**, 13203–13207
- Horiuchi, M., Baron, G. S., Xiong, L. W., and Caughey, B. (2001) *J. Biol. Chem.* **276**, 15489–15497
- Prusiner, S. B. (1996) *Trends Biochem. Sci.* **21**, 482–487
- Prusiner, S. B. (1992) in *Prion Diseases of Humans and Animals* (Prusiner, S. B., Collinge, J., Powell, J., and Anderton, B., eds) Ellis Horwood, London
- Armstrong, R. A., Lantos, P. L., Ironside, J. W., and Cairns, N. J. (2003) *J. Neural Transm.* **110**, 1303–1311
- Bruce, M. E., McBride, P. A., and Farquhar, C. F. (1989) *Neurosci. Lett.* **102**, 1–6
- Jeffrey, M., Martin, S., Barr, J., Chong, A., and Fraser, J. R. (2001) *J. Comp. Pathol.* **124**, 20–28
- Lasmezas, C. I., Deslys, J. P., Robain, O., Jaegly, A., Beringue, V., Peyrin, J. M., Fournier, J. G., Hauw, J. J., Rossier, J., and Dormont, D. (1997) *Science* **275**, 402–405
- Hetz, C., Russelakis-Carneiro, M., Maundrell, K., Castilla, J., and Soto, C. (2003) *EMBO J.* **22**, 5435–5445
- Liberski, P. P., Sikorska, B., Bratosiewicz-Wasik, J., Gajdusek, D. C., and Brown, P. (2004) *Int. J. Biochem. Cell Biol.* **36**, 2473–2490
- Puig, B., and Ferrer, I. (2001) *Acta Neuropathol.* **102**, 207–215
- Jamieson, E., Jeffrey, M., Ironside, J. W., and Fraser, J. R. (2001) *Neuroreport* **12**, 3567–3572
- Muller, W. E., Ushijima, H., Schroder, H. C., Forrest, J. M., Schatton, W. F., Rytik, P. G., and Heffner-Laue, M. (1993) *Eur. J. Pharmacol.* **246**, 261–267
- Tagliavini, F., Prelli, F., Verga, L., Giaccone, G., Sarma, R., Gorevic, P., Ghetti, B., Passerini, F., Ghibaudi, E., Forloni, G., Salmona, M., Bugiani, O., and Frangione, B. (1993) *Proc. Natl. Acad. Sci. U. S. A.* **90**, 9678–9682
- Forloni, G., Angeretti, N., Chiesa, R., Monzani, E., Salmona, M., Bugiani, O., and Tagliavini, F. (1993) *Nature* **362**, 543–546
- Etaiche, M., Pichot, R., Vincent, J. P., and Chabry, J. (2000) *J. Biol. Chem.* **275**, 36487–36490
- Chabry, J., Ratsimanohatra, C., Sponne, I., Elena, P. P., Vincent, J. P., and Pillot, T. (2003) *J. Neurosci.* **23**, 462–469
- Agostinho, P., and Oliveira, C. R. (2003) *Eur. J. Neurosci.* **17**, 1189–1196
- Brown, D. R. (1999) *J. Neurochem.* **73**, 1105–1113
- Florio, T., Thellung, S., Amico, C., Robello, M., Salmona, M., Bugiani, O., Tagliavini, F., Forloni, G., and Schettini, G. (1998) *J. Neurosci. Res.* **54**, 341–352
- Peyrin, J. M., Lasmezas, C. I., Haik, S., Tagliavini, F., Salmona, M., Williams, A., Richie, D., Deslys, J. P., and Dormont, D. (1999) *Neuroreport* **10**, 723–729
- Salmona, M., Malesani, P., De Gioia, L., Gorla, S., Bruschi, M., Molinari, A., Della, V. F., Pedrotti, B., Marrari, M. A., Awan, T., Bugiani, O., Forloni, G., and Tagliavini, F. (1999) *Biochem. J.* **342**, 207–214
- Haik, S., Peyrin, J. M., Lins, L., Rosseneu, M. Y., Brasseur, R., Langeveld, J. P., Tagliavini, F., Deslys, J. P., Lasmezas, C., and Dormont, D. (2000) *Neurobiol. Dis.* **7**, 644–656
- O'Donovan, C. N., Tobin, D., and Cotter, T. G. (2001) *J. Biol. Chem.* **276**, 43516–43523
- Turnbull, S., Tabner, B. J., Brown, D. R., and Allsop, D. (2003) *Neurosci. Lett.* **336**, 159–162
- Vaughan-Thomas, A., Gilbert, S. J., and Duance, V. C. (2000) *Investig. Ophthalmol. Vis. Sci.* **41**, 3299–3304
- Giese, A., Groschup, M. H., Hess, B., and Kretzschmar, H. A. (1995) *Brain Pathol.* **5**, 213–221
- Chishty, M. A., Strome, R., Carlson, G. A., and Westaway, D. (1997) *Neurosci. Lett.* **234**, 11–14
- Heegaard, P. M., Pedersen, H. G., Flink, J., and Boas, U. (2004) *FEBS Lett.* **577**, 127–133
- Bueler, H., Fischer, M., Lang, Y., Bluethmann, H., Lipp, H. P., DeArmond, S. J., Prusiner, S. B., Aguet, M., and Weissmann, C. (1992) *Nature* **356**, 577–582
- Due Larsen, B., and Holm, A. (1998) *J. Pept. Res.* **52**, 470–476
- LeVine, H., III (1999) *Methods Enzymol.* **309**, 274–284
- Patel, A. J., and Kingsbury, A. E. (1999) *Methods Neurosci.* **18**, 493–502
- Kunz, B., Sandmeier, E., and Christen, P. (1999) *FEBS Lett.* **458**, 65–68
- Brown, D. R. (1999) *FEBS Lett.* **460**, 559–560
- Forloni, G., Salmona, M., Bugiani, O., and Tagliavini, F. (2000) *FEBS Lett.* **466**, 205–206
- Post, K., Brown, D. R., Groschup, M., Kretzschmar, H. A., and Riesner, D. (2000) *Arch. Virol. Suppl.* **16**, S265–S273
- Raymond, G. J., and Chabry, J. (2004) in *Techniques in Prion Research* (Lehmann, S., and Grassi, J. eds) pp. 16–26, Birkhäuser Verlag AG, Basel, Switzerland
- Kayed, R., Sokolov, Y., Edmonds, B., McIntire, T. M., Milton, S. C., Hall, J. E., and Glabe, C. G. (2004) *J. Biol. Chem.* **279**, 46363–46366
- Yan, X. X., Najbauer, J., Woo, C. C., Dashtipour, K., Ribak, C. E., and Leon, M. (2001) *J. Comp. Neurol.* **433**, 4–22
- McLaughlin, B., Hartnett, K. A., Erhardt, J. A., Legos, J. J., White, R. F., Barone, F. C., and Aizenman, E. (2003) *Proc. Natl. Acad. Sci. U. S. A.* **100**, 715–720
- Buyukmihci, N., Goehring-Harmon, F., and Marsh, R. F. (1982) *J. Comp. Neurol.* **205**, 153–160
- Buyukmihci, N. C., Goehring-Harmon, F., and Marsh, R. F. (1987) *Exp. Neurol.* **97**, 201–206
- Hogan, R. N., Baringer, J. R., and Prusiner, S. B. (1981) *Lab. Invest.* **44**, 34–42
- Curtis, R., Fraser, H., Foster, J. D., and Scott, J. R. (1989) *Neuropathol. Appl. Neurobiol.* **15**, 75–89
- Foster, J. D., Fraser, H., and Bruce, M. E. (1986) *Neuropathol. Appl. Neurobiol.* **12**, 185–196
- Head, M. W., Northcott, V., Rennison, K., Ritchie, D., McCardle, L., Bunn, T. J., McLennan, N. F., Ironside, J. W., Tullio, A. B., and Bonshek, R. E. (2003) *Investig. Ophthalmol. Vis. Sci.* **44**, 342–346
- Foster, J., Farquhar, C., Fraser, J., and Somerville, R. (1999) *Neurosci. Lett.* **260**, 1–4
- Rosenblum, W. I. (2002) *Neurobiol. Aging* **23**, 225–230
- Rymer, D. L., and Good, T. A. (2000) *J. Neurochem.* **75**, 2536–2545
- Gu, Y., Fujioka, H., Mishra, R. S., Li, R., and Singh, N. (2002) *J. Biol. Chem.* **277**, 2275–2286
- Fioriti, L., Quaglio, E., Massignan, T., Colombo, L., Stewart, R. S., Salmona, M., Harris, D. A., Forloni, G., and Chiesa, R. (2005) *Mol. Cell. Neurosci.* **28**, 165–176